Supporting Information for

Dramatic Impact of the Auxiliary Ligand On the Two-Step Magnetic Relaxation Process in Dy_4(III) Single-Molecule Magnets

Kun Zhang,*[ab] Gao-Peng Li,[b] Cheng Zhang,[a] and Yao-Yu Wang*[b]

[a] School of Textile Science and Engineering, Xi'an Polytechnic University, Xi'an, 710048, P.R. China.
[b] Key Laboratory of Synthetic and Natural Functional Molecule Chemistry of the Ministry of Education, Shaanxi Key Laboratory of Physico-Inorganic Chemistry, College of Chemistry & Materials Science, Northwest University, Xi'an, 710127, P.R. China.
E-mail: zhangkun625@foxmail.com; wyaoyu@nwu.edu.cn.

Supplementary Information Contents

Page	Title
S1	**Table S1.** Crystallographic data for complexes **1** and **2**. **Figure S1.** Experimental and simulated PXRD patterns of complexes **1** and **2**.
S2	**Table S2.** Selected bond lengths (Å) and angles (°) for complexes **1** and **2**. **Table S3.** SHAPE analysis of the Dy(III) ion in complexes **1** and **2**.
S3	**Figure S2.** Crystallographic packing diagrams for complexes **1** and **2**. **Figure S3.** Field dependence of the magnetization, M, at 2, 3 and 5 K for complexes **1** and **2** plotted as M *vs.* $H\,T^{-1}$. **Figure S4.** Magnetic hysteresis loops at 1.8 K for complexes **1** and **2**.
S4	**Figure S5.** The temperature dependent in-phase (χ') ac susceptibility for complexes **1** and **2**. **Figure S6.** The temperature dependent out-of-phase (χ'') ac susceptibility for complexes **1** and **2**.
S5	**Table S4.** Relaxation fitting parameters from Least-Squares Fitting of χ(f) between 1-997 Hz data under zero dc field of complex **1**.
S6	**Table S5.** Relaxation fitting parameters from Least-Squares Fitting of χ(f) between 1-997 Hz data under zero dc field of complex **2**. **Figure S7.** Plots of ln(τ_1) versus T^{-1} for **1** and **2**.

Table S1 Crystallographic data for complexes **1** and **2**.

Complex	**1**	**2**
Formula	$C_{82}H_{82}Dy_4N_6O_{22}$	$C_{79}H_{77}Dy_4N_7O_{21}$
Fw	2153.58	2110.48
Temp (K)	150(2)	296(2)
Crystal system	Monoclinic	Monoclinic
Space group	$P2_1/c$	$P2_1/c$
a (Å)	12.9503(6)	13.120(8)
b (Å)	26.2419(12)	25.340(17)
c (Å)	11.7165(5)	12.262(8)
α (˚)	90.00	90.00
β (˚)	94.296(1)	100.908(1)
γ (˚)	90.00	90.00
Volume (Å^3)	3970.6(3)	4003(4)
Z	2	2
D_{calc} (g cm^{-3})	1.798	1.751
μ (mm^{-1})	3.799	3.766
F (000)	2104	2064
Reflections (all)	8146	6989
Reflections(> 2σ)	6539	5295
R_{int}	0.0462	0.0407
R_{sigma}	0.0379	0.0510
R_1, wR_2 ($I > 2\sigma(I)$)	0.0485, 0.1024	0.0581, 0.1451
R_1, wR_2 (all data)	0.0663, 0.1133	0.0848, 0.1624
GOF	1.085	1.123

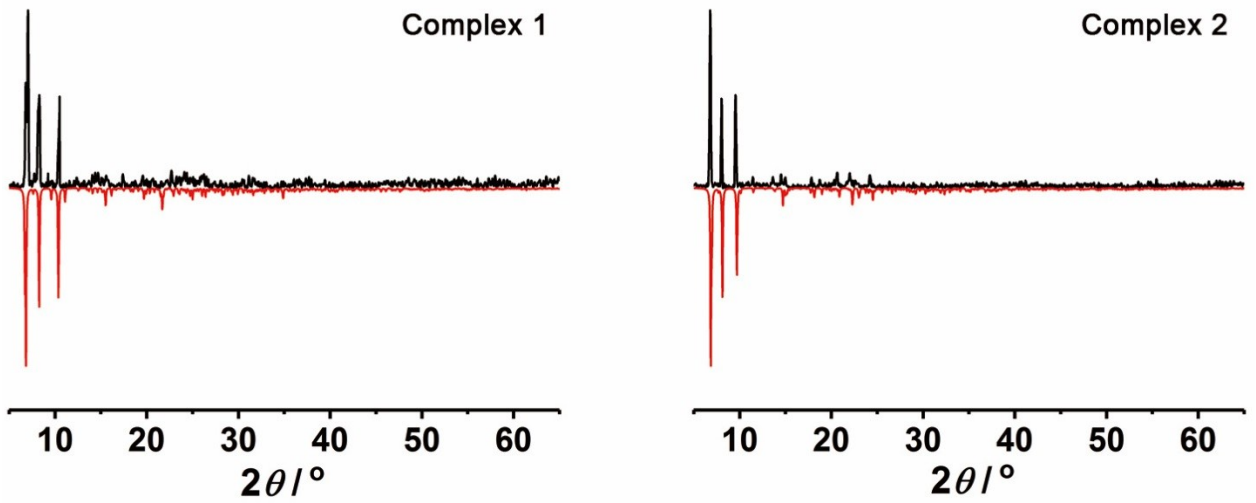

Figure S1. The experimental (black) powder X-ray diffraction and simulated patterns (red) of **1** and **2**.

Table S2 Selected bond lengths (Å) and angles (°) for complexes **1** and **2**

	1	**2**
Dy1-O1	2.353(5)	2.337(6)
Dy1-O1[a]	2.355(5)	2.362(6)
Dy1-O2	2.318(5)	2.299(8)
Dy1-O3	2.373(5)	2.362(8)
Dy1-O6	2.339(5)	2.310(7)
Dy1-O9	2.304(9)	2.303(9)
Dy1-O10	2.373(6)	2.339(9)
Dy1-N1	2.552(6)	2.506(9)
Dy2-O1[a]	2.381(4)	2.340(6)
Dy2-O2[a]	2.344(5)	2.329(7)
Dy2-O3	2.340(5)	2.343(7)
Dy2-O4[a]	2.557(6)	2.607(9)
Dy2-O5	2.205(5)	2.168(8)
Dy2-O6	2.351(5)	2.326(7)
Dy2-O8	2.360(6)	2.351(10)
Dy2-N2	2.460(6)	2.424(10)
Dy1-O1-Dy1[a]	112.6(2)	110.4(2)
Dy1-O1-Dy2[a]	109.2(2)	109.2(3)
Dy1[a]-O1-Dy2[a]	94.03(16)	94.1(2)
Dy1-O2-Dy2[a]	111.7(2)	110.9(3)
Dy1-O3-Dy2	94.63(18)	94.1(3)
Dy1-O6-Dy2	95.24(18)	95.9(2)
Dy1⋯Dy2	3.4645(6)	3.443(2)
Symmetry transformations used to generate equivalent atoms : for **1**, a: 2-x,1-y,1-z; for **2**, 1-x,1-y,1-z.		

Table S3. SHAPE analysis of the Dy(III) ion in complexes **1** and **2**

Label	Shape	Symmetry	Distortion (**1**) Dy1/Dy2	Distortion (**2**) Dy1/Dy2
OP-8	Octagon	D_{8h}	22.190/26.202	23.029/27.012
HPY-8	Heptagonal pyramid	C_{7v}	17.167/12.826	17.413/14.267
HBPY-8	Hexagonal bipyramid	D_{6h}	19.881/19.116	19.899/19.940
CU-8	Cube	O_h	18.924/17.919	19.283/17.808
SAPR-8	Square antiprism	D_{4d}	11.353/11.298	10.129/11.382
TDD-8	Triangular dodecahedron	D_{2d}	10.541/11.838	10.624/12.192
JGBF-8	Johnson gyrobifastigium J26	D_{2d}	20.169/19.209	18.716/18.931
JETBPY-8	Johnson elongated triangular bipyramid J14	D_{3h}	21.801/24.208	19.208/20.313
JBTPR-8	Biaugmented trigonal prism J50	C_{2v}	10.618/10.598	9.697/10.831
BTPR-8	Biaugmented trigonal prism	C_{2v}	10.442/12.011	9.469/12.205
JSD-8	Snub diphenoid J84	D_{2d}	12.188/12.280	10.528/12.140
TT-8	Triakis tetrahedron	T_d	19.622/17.868	20.016/17.867
ETBPY-8	Elongated trigonal bipyramid	D_{3h}	21.587/26.816	20.037/25.837

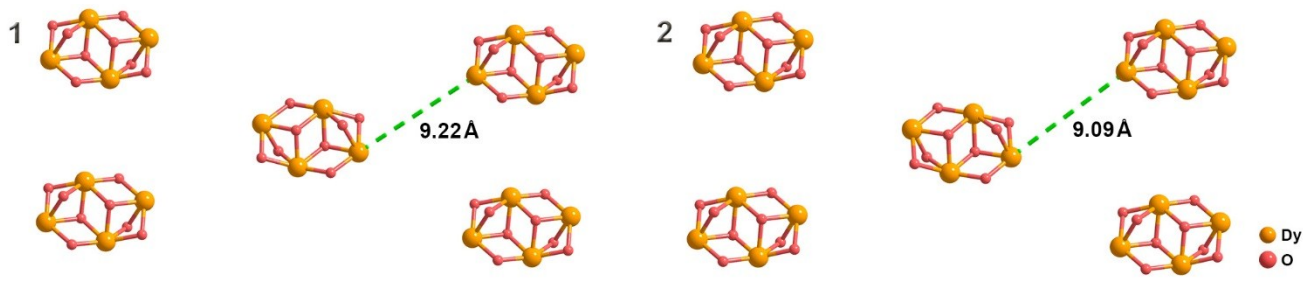

Figure S2. Crystallographic packing diagrams for complexes **1** and **2**. For clarity, only $\{Dy_4O_8\}$ cores are presented, the green dashed lines represent the shortest intermolecular Dy···Dy distances.

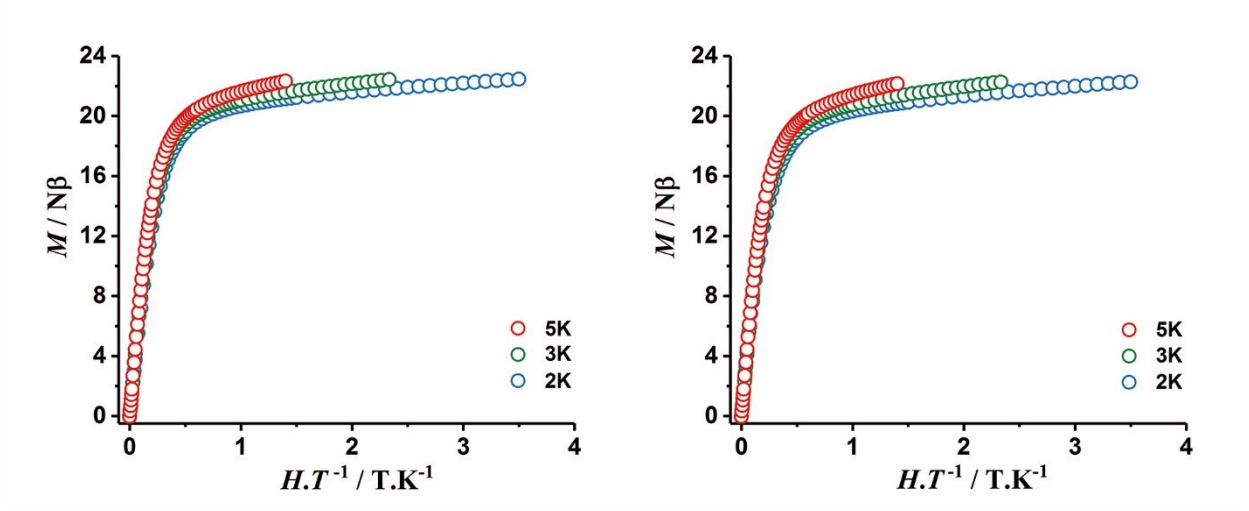

Figure S3. Field dependence of the magnetization, M, at 2, 3 and 5 K for for complexes **1** (left) and **2** (right) plotted as *M vs. H* T^{-1}.

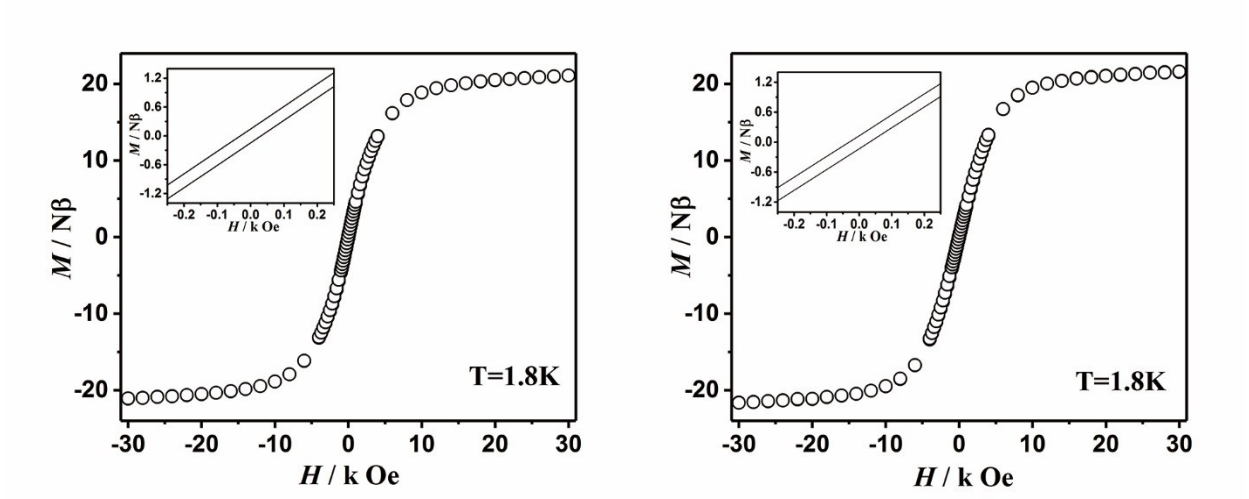

Figure S4. Magnetic hysteresis loops at 1.8 K for complexes **1** (left) and **2** (right).

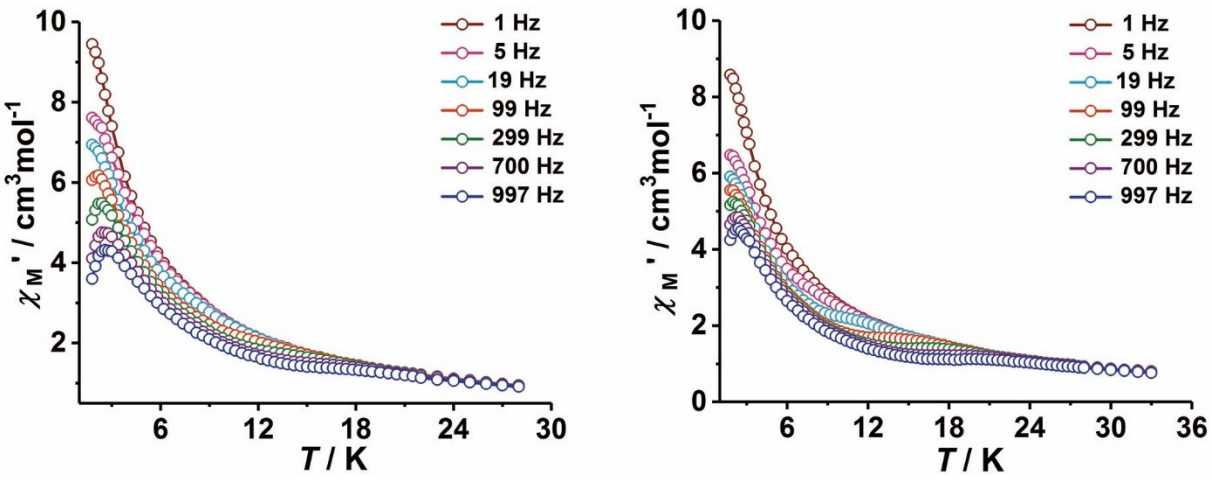

Figure S5. The temperature dependent in-phase (χ') ac susceptibility for complexes **1** (left) and **2** (right) under zero-dc field.

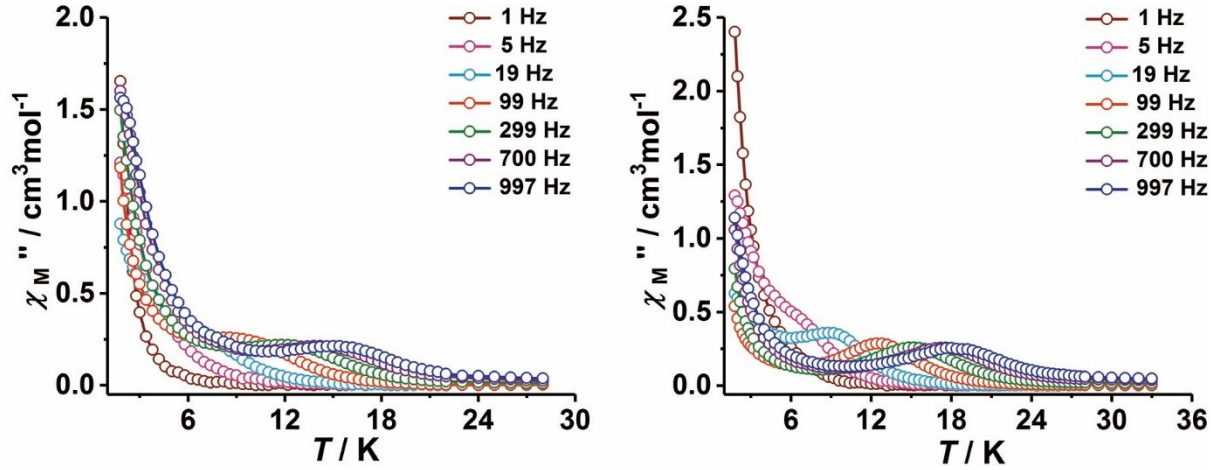

Figure S6. The temperature dependent out-of-phase (χ'') ac susceptibility for complexes **1** (left) and **2** (right) under zero-dc field.

Table S4. Relaxation fitting parameters from Least-Squares Fitting of χ(*f*) between 1-997 Hz data under zero dc field of complex **1**.

Temperature (K)	FR		SR	
	α_1	τ_1	α_2	τ_2
1.9	0.44192	1.59563E-4	0.14826	0.11497
2.2	0.44093	8.48669E-5	0.14557	0.07577
2.5	0.43461	5.46931E-5	0.14707	0.05417
2.8	0.43716	3.64184E-5	0.14113	0.04099
3.1	0.43196	2.8359E-5	0.13895	0.03229
3.4	0.42907	2.27446E-5	0.13773	0.02637
4	0.42867	1.53736E-5	0.13228	0.01862
4.5	0.43247	1.13905E-5	0.12536	0.01452
5	0.44403	8.39762E-6	0.12076	0.01167
5.5	0.45146	6.37456E-6	0.11524	0.00946
6	0.46156	4.88025E-6	0.10695	0.0078
6.5	0.46435	3.90099E-6	0.10578	0.00642
7	0.46396	3.24209E-6	0.10107	0.00531
8			0.09335	0.00362
9			0.09744	0.00243
10			0.0958	0.00162
11			0.07993	0.00112
12			0.06562	7.58592E-4
13			0.04876	5.40269E-4
14			0.02528	3.9872E-4
15			0.00536	3.05757E-4
16			2.66251E-16	2.36956E-4

Table S5. Relaxation fitting parameters from Least-Squares Fitting of χ(*f*) between 1-997 Hz data under zero dc field of complex **2**.

Temperature (K)	FR		SR	
	α_1	τ_1	α_2	τ_2
1.9	0.35249	4.06361E-5	0.22569	0.19733
2.2	0.35568	1.85126E-5	0.2278	0.14945
2.5	0.33497	1.42323E-5	0.2308	0.11968
2.8	0.32164	1.19149E-5	0.23016	0.10017
3.1	0.32087	8.69177E-6	0.22494	0.08516
3.4	0.31603	7.41691E-6	0.22037	0.07499
4	0.31614	5.58505E-6	0.20901	0.06051
4.5	0.32077	4.51658E-6	0.19909	0.05193
5	0.32594	3.77736E-6	0.18675	0.04482
5.5	0.32806	3.28301E-6	0.17493	0.03856
6	0.33455	2.86765E-6	0.15914	0.03283
6.5	0.33266	2.6506E-6	0.14497	0.0278
7	0.34650	2.31952E-6	0.1276	0.02323
7.5			0.1159	0.01917
8			0.10082	0.01556
9			0.07917	0.01002
10			0.06486	0.00625
11			0.05768	0.00388
12			0.05474	0.00241
13			0.04904	0.00154
14			0.0383	0.00102
15			0.02509	6.98032E-4
16			0.01149	4.96157E-4
17			0.00266	3.60033E-4
18			0.00377	2.62095E-4
19			9.20311E-8	2.00865E-4

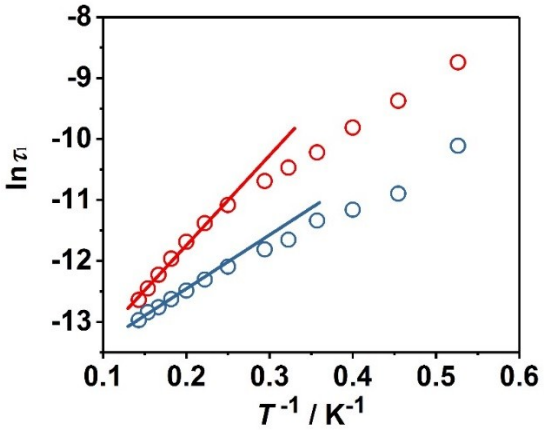

Figure S7. Plots of ln(τ_1) versus T^{-1} for **1** and **2** (**1**, red circles; **2**, blue circles), where τ_1 is the relaxation time for the fast relaxation process, *T* refers to the temperature (K). The solid lines represent the best fits to the Arrhenius law of the thermally activated region.